Remote Sensing of Environment 223 (2019) 82–94

Contents lists available at ScienceDirect

Remote Sensing of Environment

journal homepage: www.elsevier.com/locate/rse

A comprehensive validation of the SMAP Enhanced Level-3 Soil Moisture product using ground measurements over varied climates and landscapes

Runze Zhang, Seokhyeon Kim*, Ashish Sharma

School of Civil and Environmental Engineering, University of New South Wales, Sydney, NSW 2052, Australia

ARTICLE INFO

Keywords:
SMAP
Surface soil moisture
Validation

ABSTRACT

This study presents a comprehensive validation of the Soil Moisture Active Passive (SMAP) mission Enhanced Level-3 radiometer soil moisture (SM) product (Version 2) over 3 years from April 1, 2015 to March 31, 2018 using extensive ground measurements from sparse networks covering a range of physical and climatological regimes. Using a common spatial resolution, soil moisture retrievals from the descending (6:00 AM) and ascending (6:00 PM) overpasses were assessed based on static conditions such as the climate zone, soil property and land cover. Then validation considering performance with respect to dynamic attributes such as soil wetness, vegetation density and land surface temperature was reported. Given the above six parameters are cross-correlated, the quality of the SMAP enhanced products was further evaluated based on pairwise factors.

Overall, higher accuracy was noted over zones where the soil organic carbon is low, the vegetation density is relatively sparse, locations in the temperate and arid climate zones, and the mean LST is high. Results also indicate that the descending (AM) and ascending (PM) products exhibit mean temporal correlation over the ground stations equaling 0.667 and 0.651, and mean unbiased root mean square error (ubRMSE) equaling 0.055 and 0.054 m^3/m^3 respectively which is close to the ubRMSE requirement of the SMAP mission, 0.04 m^3/m^3. While the ascending (PM) SM retrievals have been frequently excluded from applications due to its poor performances reported form validation studies, these comparable performances between the two products suggest that the ascending (PM) SM retrievals can be an additional data source. Based on the results here, it can be concluded that there is room for improving the SMAP product especially in areas of the world with very dense vegetation and average to low land surface temperatures.

1. Introduction

Soil moisture (SM) is an important component of the hydrological cycle and land-atmosphere interactions (Chen et al., 2011; Koster et al., 2004; Li et al., 2018). SM controls infiltration, surface overland flow, and plays a vital role in partitioning energy fluxes (Beven and Fisher, 1996; Das and Paul, 2015). Due to its relevance, SM has been recognized as an Essential Climate Variable (ECV) by the Global Climate Observing System (GCOS) (GCOS, 2006). Accurate measurement of SM hence has significant importance in a range of applications from flood prediction to drought monitoring (Engda and Kelleners, 2016; S. Kim et al., 2018).

Microwave remote sensors have been considered as an effective tool to measure the globally spatial distribution of the soil water content given its uniquely strong relationship with the dielectric constant of the soil (Petropoulos et al., 2015). In addition to all-weather operations and continuous measurements during day and night, passive microwave sensors exhibit greater temporal resolution and lower impacts of surface roughness disturbances while active microwave sensors show higher quality in spatial resolution (Bertoldi et al., 2014; Kornelsen and Coulibaly, 2013; Ulaby et al., 1986).

To incorporate advantages of both active and passive microwave remote sensors (Entekhabi et al., 2010a), the Soil Moisture Active Passive (SMAP) satellite mission was launched on January 31, 2015, by the National Aeronautics and Space Administration (NASA) with a 3-day global coverage, the L-band radiometer and L-band radar onboard are dedicated to collect and provide the high-resolution mapping of global SM and the freeze-thaw state of soil (Chan et al., 2016; Srivastava et al., 2016). Due to the low frequency at L-band (1.41 GHz), negligible atmospheric effects and the deeper penetrating capability over the vegetation canopy occur, leading to a higher accuracy of the signals received (Kerr et al., 2016; Wigneron et al., 2017). Additionally, use of the anti-interference hardware and kurtosis-based algorithms help reduce the radio frequency interference (RFI) caused by the

* Corresponding author.
E-mail address: seokhyeon.kim@unsw.edu.au (S. Kim).

https://doi.org/10.1016/j.rse.2019.01.015
Received 20 November 2018; Accepted 12 January 2019
0034-4257/

Table 1
Summary of data used in this study.

Data	Data source and/or product name	Resolution (temporal/spatial)	Unit
Satellite soil moisture	SMAP enhanced L3 soil moisture products (SPL3SMP_E, Version 2)	Daily/9 km	m^3/m^3
In-situ soil moisture	ISMN	Hourly/point	m^3/m^3
Reanalysis soil moisture	MERRA-2 top soil layer soil moisture consent SFMC (M2T1NXLND)	Hourly (time-averaged)/0.5° × 0.625°	m^3/m^3
Climate zone	Peel et al. (2007)	−/0.25°	–
Soil property	SMAP Microwave Radiative Transfer Model: Soil class (SPL4SMLM)	−/9 km	–
Land cover	MODIS (MCD12Q1)	Yearly/0.05°	–
Vegetation	SMAP Vegetation Water Content (SPL3SMP_E)	Daily/9 km	kg/m^2
Land surface temperature	SMAP Land Surface Temperature (SPL3SMP_E)	Daily/9 km	K

anthropogenic activities (Piepmeier et al., 2014). Owing to an irrecoverable malfunction that happened to the radar in July 2015, the SMAP data released have been derived from brightness temperatures collected by the L-band radiometer alone.

The SMAP products have been widely validated and/or applied since the relevant datasets were released in April 2015 (Burgin et al., 2017; Chan et al., 2018; Chan et al., 2016; Chen et al., 2017; Colliander et al., 2017a; Colliander et al., 2017b; Colliander et al., 2018; Jackson et al., 2018; S. Kim et al., 2018; Pan et al., 2016; Zhang et al., 2017). The related validation studies can be classified into five categories according to their reference dataset sources. These are post-launch field campaigns, comparisons with other remote-sensed products, use of core validation sites, use of sparse ground networks, and comparisons with land surface model simulations. Recently, the SM retrievals from the latest version of SMAP Level-2 (L2) SM products and SMAP enhanced L2 SM products spanning from April 1, 2015, to March 31, 2018 have been separately compared against the ground-point observations from the core validation sites along with the sparse network to assess the SMAP retrieval performance via statistical metrics (Jackson et al., 2018). Zhang et al. (2017) have evaluated the accuracy of SMAP Level-4 (L4) surface SM retrievals and Advanced Microwave Scanning Radiometer 2 (AMSR2) Level-3 (L3) descending products (April 2015 to March 2016) using in-situ measurements from two American monitoring sites. Colliander et al. (2017a) have conducted pairwise validations between SMAP Level-1 (L1) and L2 retrievals and ground measurements within the zones of the post-launch field campaign in the United States applying the airborne Passive/Active L-band Sensor (PALS) as a means of assessing the product where SM spatial distributions are highly uneven. H. Kim et al. (2018) have validated three satellite products with the period from April 2015 to December 2016, including the SMAP Enhanced L2 descending products, Advanced Scatterometers (ASCAT) surface SM products and AMSR2 Land Parameter Retrieval Model (LPRM) datasets using model-based SM as ground truth allowing assessment under different vegetation fractions and land cover conditions. Colliander et al. (2018) have compared the performance of the SMAP enhanced L2 descending products with a 9 km spatial resolution processed by Backus-Gilbert interpolation with using ground observations over 9 km and 33 km domains from the core validation sites.

It must be noted that past validation studies have not focused on the performance of SMAP products under varied physical and climatological conditions given the relatively short study periods that have been available. To address this, our study aims to evaluate the performance of the recently released SMAP Enhanced L3 passive SM product (Version 2) for the first 3 years of the mission (April 1, 2015– March 31, 2018) and ascertain reasons for variations across a range of conditions including climate zone, soil property, land cover, soil wetness, vegetation density and land surface temperature. These selections have been based on the tau-omega model (Mo et al., 1982) which forms the theoretical basis to retrieve soil moisture from passive microwave and is also being used for the SMAP L2 passive microwave soil moisture algorithm. In addition to soil wetness itself, soil property, land surface temperature, and vegetation water content serve as inputs in the process of generating the SMAP L3 products (Entekhabi et al., 2014), and land cover is associated with several significant parameters for the SM retrievals even though it is not a direct input for the tau-omega model (Kim, 2013). Notably, the climate zone is not directly associated with the parameters used in SM retrieval algorithms and has hence been chosen as an indicator considering the role climatology plays in retrieval accuracy. Globally distributed ground measurement data from the sparse network are used in this validation. In addition, consistent with the validation of L2 products by Chan et al. (2018), descending and ascending L3 products have also been compared. Given the above six parameters are cross-correlated, the quality of the SMAP enhanced products has been further evaluated based on the pairwise factors.

This paper is structured as follows. Section 2 briefly presents the relevant datasets developed and the procedures used to pre-process the data in this study. In Section 3, the assessment metrics adopted are described. This is followed by a presentation and a detailed discussion of the results (Section 4). Finally, conclusions are presented in Section 5.

2. Data and data processing

Datasets used in this study over the 3-year study period (April 1, 2015– March 31, 2018) are summarised in Table 1. These include the SMAP Enhanced L3 Radiometer Global Daily 9 km EASE-Grid Soil Moisture dataset (SPL3SMP_E, Version 2), globally distributed ground measurements obtained from the International Soil Moisture Network (ISMN) (Dorigo et al., 2011) as the reference data, the volumetric soil moisture content in the top layer (0–0.05 m) (SFMC) of the Modern-Era Retrospective Analysis for Research and Applications Land version 2 reanalysis (MERRA-2) (Global Modeling and Assimilation Office (GMAO), 2015), and six physical and climatological indicators, climate zone, soil property, land cover, soil wetness, vegetation density and land surface temperature, which affect soil moisture retrieval significantly (De Lannoy et al., 2014; Entekhabi et al., 2014; Kim, 2013; Kim et al., 2015; Schmugge, 1980). In addition to this, in cases where there exist two or more ground stations in a 0.1° × 0.1° pixel, MERRA-2 SFMC has been additionally used for representing areal representativeness of each station in the grid cell, details for which are provided in the following Section 2.1.2.

Of the six physical and climatological conditions, the first three conditions, climate zone (CZ), soil property (SP) and land cover (LC), are considered as static conditions and results are presented in Section 4.2. The remaining indicators (soil wetness (SW), vegetation density (VD) and land surface temperature (LST)) present dynamic conditions which vary with the soil moisture being estimated, results being presented in Section 4.3. It should be noted that a geographic coordination with spatial resolution of 0.1° × 0.1° pixels was commonly used throughout this study by resampling all data having various spatial resolutions using bilinear interpolation unless otherwise stated.

2.1. Soil moisture data

2.1.1. SMAP soil moisture

The recently released SMAP Enhanced L3 Radiometer Global Daily 9 km EASE-Grid Soil Moisture (SPL3SMP_E, Version 2), hereinafter referred to as SMAP L3, was selected in the assessments reported next. The SMAP L3 product is a daily global product that presents volumetric surface SM (0–5 cm, m^3/m^3) and brightness temperature in Kelvin (K) retrieved by the SMAP L-band radiometer (1.41 GHz) on the 9 km global cylindrical Equal-Area Scalable Earth (EASE) Grid 2.0 (Brodzik et al., 2012). This enhanced L3 product is a daily composite of SMAP enhanced L2 half-orbit products, where the L3 ascending and descending products are derived separately by only considering the enhanced L2 SM products acquired (Chan, 2016; O'Neill et al., 2016a). The SMAP enhanced L2 SM product is derived from the SMAP Enhanced L1 Gridded Brightness Temperature Product (L1CTB_E) (posted at 9 km grid cell) based on Backus-Gilbert optimal interpolation technique (Chan et al., 2018; Colliander et al., 2018; O'Neill et al., 2016a).

Comparing with the previous version of the SMAP enhanced products, three changes were introduced in the Version 2 product (Jackson et al., 2018). In addition to the water body correction and recalibration of the L1 brightness temperature products, the formulation used to calculate the effective soil temperatures has also been modified to reduce the mean differences between the satellite SM retrievals and in-situ SM measurements. As a result, it has been shown that the Version 2 product significantly improved in terms of bias. Although the nominal spatial extent of the SMAP radiometer is 36 km × 36 km and the SMAP enhanced product are posted on the 9 km pixel, the contributing domain of the SMAP enhanced product is 33 km × 33 km. (Chan et al., 2018; Chan et al., 2016; Colliander et al., 2018; O'Neill et al., 2016a). This SMAP enhanced L3 product came from the NASA National Snow and Ice Data Center Distributed Active Archive Center (NSIDC DAAC, http://nsidc.org/data/smap/smap-data.html).

While the descending (6 AM local time) SM retrievals are commonly adopted by researchers due to their relatively higher quality than the ascending (6 PM local time) data because of more favorable thermal equilibrium conditions between vegetation and near surface soil (De Jeu et al., 2008), both products were used in the assessments reported here. To ensure stable assessments, only the SMAP datasets not affected by the following filters were used (Bindlish et al., 2015; Choudhury et al., 1982; O'Neill et al., 2016b): (1) grids where the open water fraction is larger than 10%; (2) grids where the frozen condition (LST < 273.15 K) fraction is > 10%; (3) highly dense vegetation areas (vegetation water content > 5 kg/m^2); (4) not recommended by the SMAP retrieval quality flag.

2.1.2. In-situ soil moisture

To effectively assess the SMAP L3 product, in-situ observations from the ISMN were used (Dorigo et al., 2011). The ISMN, maintained by the Vienna University of Technology, is a centralized data system that collects and disseminates globally harmonized in-situ SM measurements from diverse validation campaigns and operational networks, and the ISMN currently (October 2018) consists of 2439 ground stations from 59 networks mainly distributed over the United States and Europe. In addition, the ISMN data are freely available for all users through the data access website (https://ismn.geo.tuwien.ac.at/data-access/) and these data have been extensively applied in a large number of validation studies (Dorigo et al., 2017; H. Kim et al., 2018; Ochsner et al., 2013).

It should be noted that the in-situ stations used for evaluating the performance of the SMAP L3 product are mostly from the sparse networks which often have only one station distributed over one satellite footprint (Chan et al., 2018; Jackson et al., 2018). Even though one station can continuously provide reliable surface SM measurements (0–5 cm), these observations at a point are hardly able to reflect the SM variations for such a large area covered by the SMAP radiometer scans are significant. Additionally, the spatial mismatch between the satellite products and the sparse network can affect the ability of the approach to detect the performance differences leading to a large amount of noise. Given that, it can be expected that the quality of the SM retrievals evaluated using the ground observations from the sparse network is not as accurate and reliable as that assessed using the in-situ measurements from the core validation sites (CVSs). Based on the statistical metrics, however, the results of the performance evaluation of the SMAP enhanced products using the sparse networks showed up slightly inferior but very similar to the CVS results where the average unbiased root mean square error is slightly lower than 0.04 m^3/m^3 (Jackson et al., 2018). More importantly, sparse networks involve a large number of stations with the coverage of diverse environments so that validating the SM retrievals using sparse networks could be more aligned with the objective of this study to evaluate the performance of SMAP SM products over varied landscapes and climates.

There exist systematic differences between the satellite and ground data resulting from the spatial representativeness, different measurement depths, uncertainties in the land surface parameterization through the soil moisture retrieval algorithm and differences in sensitivity against rainfall events at the same pixel (Colliander et al., 2017a; Crow et al., 2012; Parinussa et al., 2011). To minimize these systematic differences while keeping data quality acceptable, the following filtering criteria (Dorigo et al., 2015) were applied for the in-situ SM data from the whole operating networks: (1) only stations that measure SM at a shallowest depth < 10 cm were selected; (2) the stations for which topographic complexity (TC) and wetland fraction (WF) are smaller than 10%, were chosen, the TC and WF data being available from the European Space Agency Climate Change Initiative (ESA CCI) (Chung et al., 2018); (3) the data identified as 'good' in the quality flags of the ISMN were adopted (Dorigo et al., 2013); (4) for any pixel, the in-situ SM measured closest to the AM and PM scan time of SMAP were retained; (5) when two or more stations locate within a grid cell, only one station is considered as the most representative for the pixel. This is because taking account of all datasets within one pixel in validation would lead to an unevenly high weight for the accuracy assessment of SM retrievals in that pixel in comparison to the grid with one station (Dorigo et al., 2015). Therefore, following the method used in Dorigo et al. (2015), the areal representativeness of the station depends upon the average of the correlation between the in-situ SM and the SMAP enhanced L3 SM data and the correlation between the in-situ SM and the MERRA-2 SFMC data. The stations with the highest mean correlation values for each pixel can be retained. Notably, those selected stations do not necessarily have the highest correlation with the SMAP enhanced L3 SM data. Here, daily values at each grid cell were selected from the hourly time series of the MERRA-2 SFMC data, which are temporally closest to the SMAP scan time over the grid on the day. Furthermore, to ensure statistical robustness, stations having at least 100 paired observations were used in this study. Consequently, only 191 ground stations from 13 networks were retained and used out of 1276 stations in 21 networks, which are mostly concentrated over the United States and Europe as presented in Fig. 1 and Table 2.

2.2. Static conditions

Static conditions refer to those changing relatively slow allowing assumptions of stationarity to be imposed over the study period. Here, these present assessments for climate zone (CZ), soil property (SP) and land cover (LC). Assessments were performed by forming a range of statistical metrics (see Section 3) using the SMAP L3 products and ground measurements at the station locations presented in Fig. 1. Given the global distribution of metrics and global classification maps for the static conditions (Table 1), grid cells were grouped according their static conditions separately. Further details for each classification are described in the following Subsections 2.2.1 to 2.2.3.

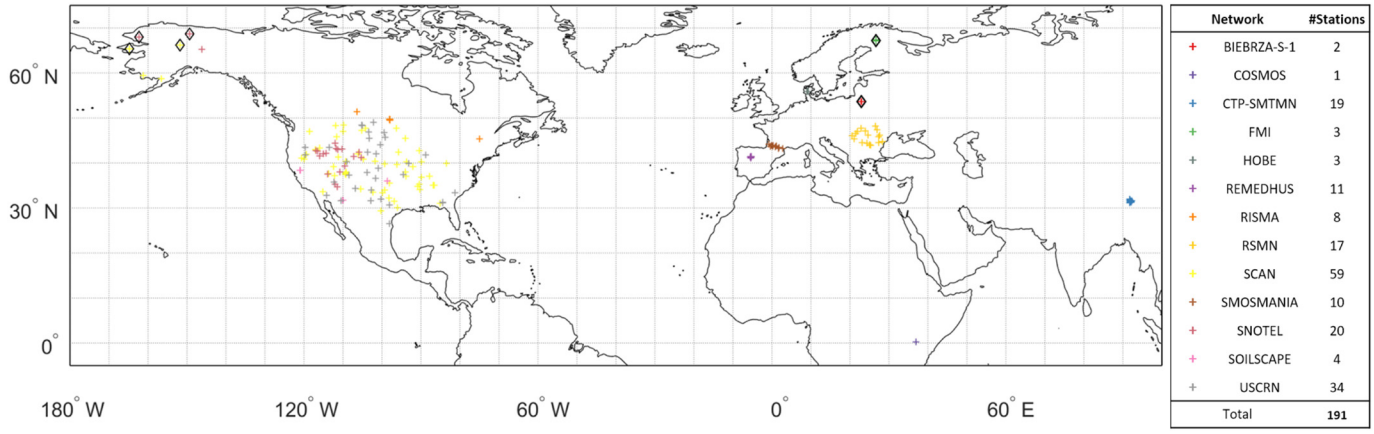

Fig. 1. The global distribution of 191 ground stations used in this study. The stations with diamond marks distributed over Alaska, and Northern Europe have high soil organic carbon > 8.72% (De Lannoy et al., 2014) (see Section 2.2.2).

Table 2
Summary of ground stations used for study.

Network	Country	No. of stations	Depth[a] (cm)	References
BIEBRZA-S-1	Poland	2	5.00	http://www.igik.edu.pl/en
COSMOS	USA	1	10.00	Zreda et al. (2008)
CTP-SMTMN	China	19	5.00	Yang et al. (2013)
FMI	Finland	3	5.00	http://fmiarc.fmi.fi/
HOBE	Denmark	3	5.00	Bircher et al. (2012)
REMEDHUS	Spain	11	5.00	Sanchez et al. (2012)
RISMA	Canada	8	5.00	Ojo et al. (2015)
RSMN	Romania	17	5.00	http://assimo.meteoromania.ro
SCAN	USA	59	5.08	http://www.wcc.nrcs.usda.gov/
SMOSMANIA	France	10	5.00	Albergel et al. (2008)
SNOTEL	USA	20	5.08	Leavesley et al. (2008)
SOILSCAPE	USA	4	5.00	Moghaddam et al. (2010)
USCRN	USA	34	5.00	Bell et al. (2013)
Total		191		

[a] Referred to station static variables from the ISMN.

2.2.1. Climate zone

In this study, the updated Koppen–Geiger climate classification (Peel et al., 2007) was used for assessing how the climate zone (CZ) affects the performance of the SM retrievals. The updated climate classification delineates a global distribution of different climatic types based on monthly temperature and precipitation station records (1901–2000) from the Global Historical Climatology Network (GHCN) version 2.0 dataset. The climate types in this map fall into five primary types (i.e. Tropical, Arid, Temperate, Cold, and Polar) and 30 possible sub-classes. This study only used the five primary climate types for the assessments. It should be noted that 18 out of 19 stations in the CTP-SMTMN network (Yang et al., 2013) are distributed over the Tibetan Plateau (> 4400 m above sea level) and belong to Polar climate zone (ET, Polar-Tundra, temperature of the hottest month > 0 °C) by the updated Koppen–Geiger climate classification (https://people.eng.unimelb.edu.au/mpeel/koppen.html).

2.2.2. Soil property

This study used an updated soil texture map suggested by De Lannoy et al. (2014) for assessing the SMAP performance with relation to soil property (SP). This map is based on the Harmonized World Soil Databank version 1.21 (HWSD) (Nachtergaele and Batjes, 2012) and the high-resolution State Soil Geographic (STATSGO2) (NRCS Soil Survey Staff, 2012), with the former covering most of the world and the latter containing information for the United States. Given the high sensitivity of soil dielectric constants with soil moisture and the documented importance of organic matter content in the SM estimation (Kay et al., 1997; Letts et al., 2000; Manns et al., 2017), the soil texture map consists of four primary categories depending on amounts of organic carbon and is divided into 253 subclasses with associated hydraulic properties.

As the soil texture map has been also used for generating the SMAP L4 Surface and Root Zone Soil Moisture data product, the dataset is available as one of SMAP products (SPL4SMLM) and can be obtained from the NSIDC DAAC as well. Notably, the soil classification used here only involved the four categories by the content of organic carbon, termed as OC1 to OC4 as described in Table 3.

2.2.3. Land cover

In this study, a Moderate Resolution Imaging Spectroradiometer (MODIS)-derived land cover (LC) map was used for assessing effects of LC on the performance of the SMAP L3 product. This yearly MODIS LC product is named as MCD12C1 (Version 051) (Friedl et al., 2010) and its spatial resolution is 0.05° × 0.05°. Among the yearly datasets from 2001 to 2012, the LC map from 2012 was selected which is freely available on the NASA Earthdata website (https://earthdata.nasa.gov/). The MCD12C1 product incorporates the 17-class International Geosphere Biosphere Program (IGBP) that are simplified as 6 primary classes except for Permanent wetlands, Permanent snow and ice, and Water (Table 4). This study only used the 6 primary LC classes for the assessments.

2.3. Dynamic conditions

Dynamic assessments were performed for conditions that vary in time, which are soil wetness (SW), vegetation density (VD) and land surface temperature (LST). In this study, cross-correlation analyses were implemented by investigating how the SM performance is affected by one of the three dynamic factors which is conditioned by CZ. By doing so, effects on the SM retrieval by the dynamic factors may be more reliably describe. This kind of research can also be extended to consider more than two factors which may be helpful to interpret the

Table 3
Primary soil classes by organic carbon contents (De Lannoy et al., 2014).

Primary classes	Organic carbon (OC, %)	Subclass number
OC1	$0 \le OC < 0.40$	1–84
OC2	$0.40 \le OC < 0.64$	85–168
OC3	$0.64 \le OC < 8.72$	169–252
OC4	$OC \ge 8.72$	253

Table 4
IGBP land cover classification (Friedl et al., 2010).

IGBP classes	Specific classification	Primary classification
1	Evergreen needleleaf forest	Forest
2	Deciduous needleleaf forest	
3	Evergreen broadleaf forest	
4	Deciduous broadleaf forest	
5	Mixed forests	
6	Closed shrublands	Shrublands
7	Open shrublands	
8	Woody savannas	Woodlands
9	Savannas	
10	Grasslands	Grasslands
11	Permanent wetlands	/
12	Croplands	Croplands
14	Cropland/natural vegetation mosaics	
13	Urban and built-up land	Unvegetated
16	Barren or sparsely vegetated	
15	Permanent snow and ice	/
17	Water	

results in greater depth, however, this was not considered here to maintain simplicity of presentation and interpretation. Instead, more assessment results conditioned by the SP and LC are provided in Supplementary Information for further consideration.

For the assessments, the following procedures were adopted: (1) a dataset at each ground station was prepared, including time series of in-situ measurements (first column), the SMAP L3 retrievals (second column), one of the dynamic conditions (third column), and the climate zone identifiers (fourth column), (2) the 4-column datasets over all stations were sequentially appended to each other, creating an integrated 4-column dataset, (3) the integrated 4-column dataset was separated by one of the climate zone identifiers in the fourth column, (4) the separated 4-column dataset was sorted in an ascending order along the selected dynamic condition in the third column, (5) the sorted 4-column dataset was divided into 10 segments by deciles of the selected dynamic condition, (6) the four statistical metrics described in Section 3 were sequentially calculated along with the 10 data segments. Then these results were reported in Section 4 as line charts for the descending (AM) and ascending (PM) products. The three dynamic conditions used are briefly described through the following Sections 2.3.1 to 2.3.3.

2.3.1. Soil wetness

As mentioned in Section 2.1.2, the ground observations closest to SMAP scanning time were retained. These in-situ measurements over the 191 stations were used for the soil wetness condition through the data processing procedure (1) to (6) described in the previous section.

2.3.2. Vegetation density

The vegetation water content (VWC) data, which is one of ancillary datasets of the SMAP L3 products, was used for representing the density of vegetation over the area. The VWC, expressed in units of kg/m^2, assists in accurately estimating SM in the SMAP retrieval algorithm. As the VWC cannot be directly measured from currently available sensors, a secondary-derivation method based upon Hunt et al. (1996) is used, which takes the measurable and highly correlated parameter, the Normalized Difference Vegetation Index (NDVI), and the LC variability into consideration (Chan et al., 2013).

2.3.3. Land surface temperature

The SMAP land surface temperature (LST) ancillary dataset (SMAP Algorithm Development Team and SMAP Science Team, 2015), referred to the globally effective soil temperature product that presents the average soil temperatures within the surface layers (0–5 cm), was selected here. This ancillary dataset relies on the NASA Goddard Earth Observing System Model, Version 5 forward process system (GEOS-5) soil temperature output products from NASA Goddard Modeling and Assimilation Office (GMAO).

3. Assessment metrics

Four conventional statistical metrics were applied for the validation, which are bias, root mean square error (RMSE), unbiased root mean square error (ubRMSE) and time series correlation (R) (Entekhabi et al., 2010b). If the surface SM products measured by the ground stations and estimated by the satellite were denoted as θ_{true} and θ_{est} (vectors), respectively, the bias, RMSE, ubRMSE and R can be written as Eqs. (1) to (4) where E […] presents the arithmetic mean of the data.

$$\text{bias} = E[\theta_{est}] - E[\theta_{true}] \tag{1}$$

$$\text{RMSE} = \sqrt{E[(\theta_{est} - \theta_{ture})^2]} \tag{2}$$

$$\text{ubRMSE} = \sqrt{\text{RMSE}^2 - \text{bias}^2} \tag{3}$$

$$R = \frac{E[(\theta_{est} - E[\theta_{est}])(\theta_{true} - E[\theta_{true}])]}{\sigma_{est}\sigma_{true}} \tag{4}$$

4. Results and discussion

In this section, assessment results of the SMAP Enhanced L3 SM product are presented through the following subsections using box plots, line charts and tables. Section 4.1 includes overall performance of the AM and PM retrievals, and Sections 4.2 and 4.3 show assessment results using the static and dynamic conditions respectively.

The blue and red colors in Figs. 2 to 8 indicate the descending (AM) and ascending (PM) product results respectively. Arithmetic mean (m) and standard deviation (std) values of the four metrics (Section 3) for each assessment are presented in Tables 5 to 8 as a form of "m ± std" for simple comparisons between the AM and PM products along with the static conditions. Additionally, *p* values from paired-sample *t*-tests between the calculated metrics of the AM and PM products are presented to check statistical significances for rejecting a null hypothesis that mean values of the two sets of metrics are same. Simply stated, it is harder for the null hypothesis to be rejected with larger *p* values.

4.1. Overall performance of AM and PM products

The box plots in Fig. 2 and Table 5 present overall performance results for the AM and PM products in terms of the four metrics.

Overall performances of the AM and PM products can be summarised as follows. First, the bias and RMSE of the AM data are similar with those of the PM data as presented in Fig. 2a–b and as per the large *p* values in Table 5. The slightly positive bias is consistent with the evaluation results using sparse networks for the L2 SMAP Enhanced (L2SMP_E) Version 2 data products, but mean bias for the products using CVSs and the SMOS products using sparse networks were generally presented as negative (Al-Yaari et al., 2017; Jackson et al., 2018). Second, as shown in Fig. 2c, with the ubRMSEs, removing the biases from the RMSEs bring the results closer to the SMAP mission requirement, $0.04\ m^3/m^3$. Lastly, the R of the AM data is imperceptibly better than that of the PM data with a *p* value of 0.028 (Fig. 2d). Generally, the AM product shows better performance than the PM product consistent with the previous validation results (Chan, 2016; Chan et al., 2018). Given the thermal equilibrium between vegetation canopy and land surface in the morning are better matched to the assumptions in SM retrieval algorithms, the higher quality of AM retrieval is in line with exiting research (Chan et al., 2018; De Jeu et al., 2008; O'Neill et al., 2016b). However, it should be noted that the differences in the performances between the AM and PM products are not so contrasted and similarly, the PM retrievals without significant errors as expected have also been found in the early results from the Soil Moisture and Ocean

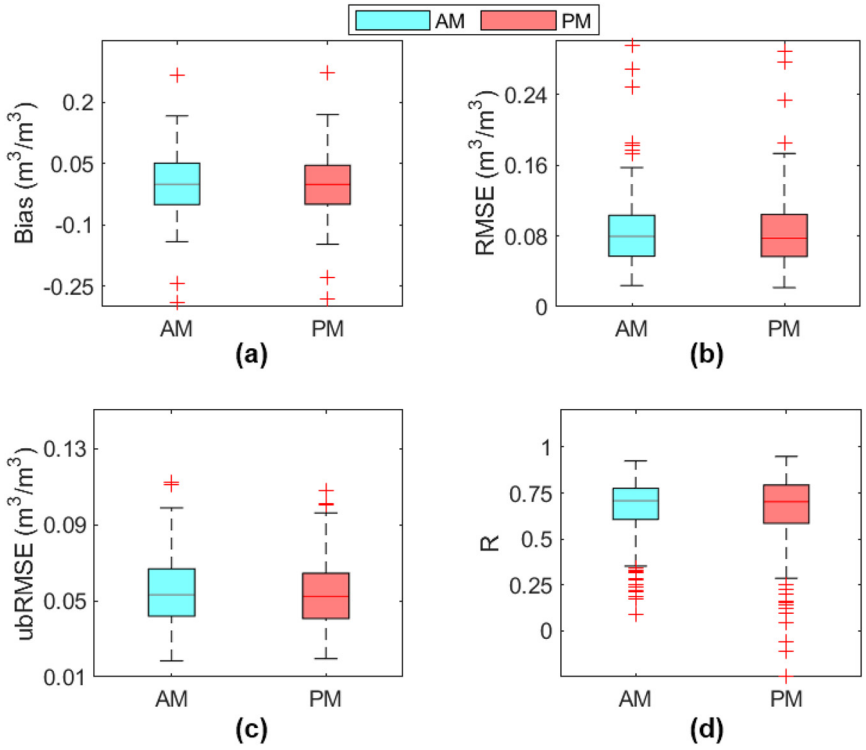

Fig. 2. Boxplots showing performance metrics for the AM and PM products in terms of (a) bias, (b) RMSE, (c) ubRMSE and (d) R. (For interpretation of the references to color in this figure, the reader is referred to the web version of this article.)

Salinity (SMOS) products (Jackson et al., 2012; O'Neill et al., 2016b). Therefore, the PM product may also be valuable for various applications together with the AM product.

4.2. Assessment results for static conditions

4.2.1. Climate zones

Each validation metric has been assigned to a primary climate class as shown in Fig. 3 and Table 5 where the tropical area was excluded

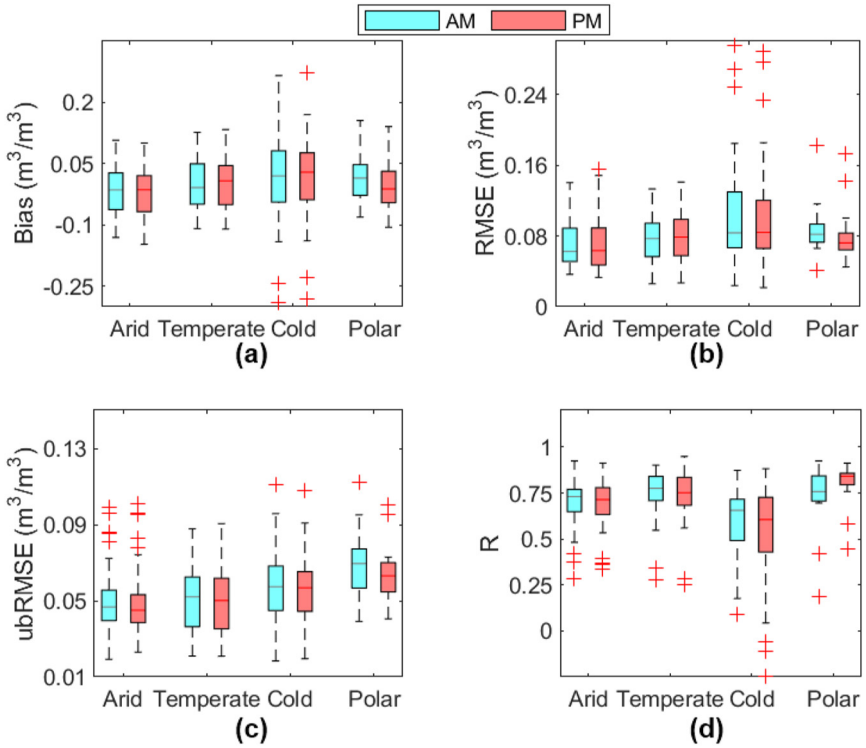

Fig. 3. Performance metrics for primary climate zones in terms of (a) bias, (b) RMSE, (c) ubRMSE and (d) R. (For interpretation of the references to color in this figure, the reader is referred to the web version of this article.)

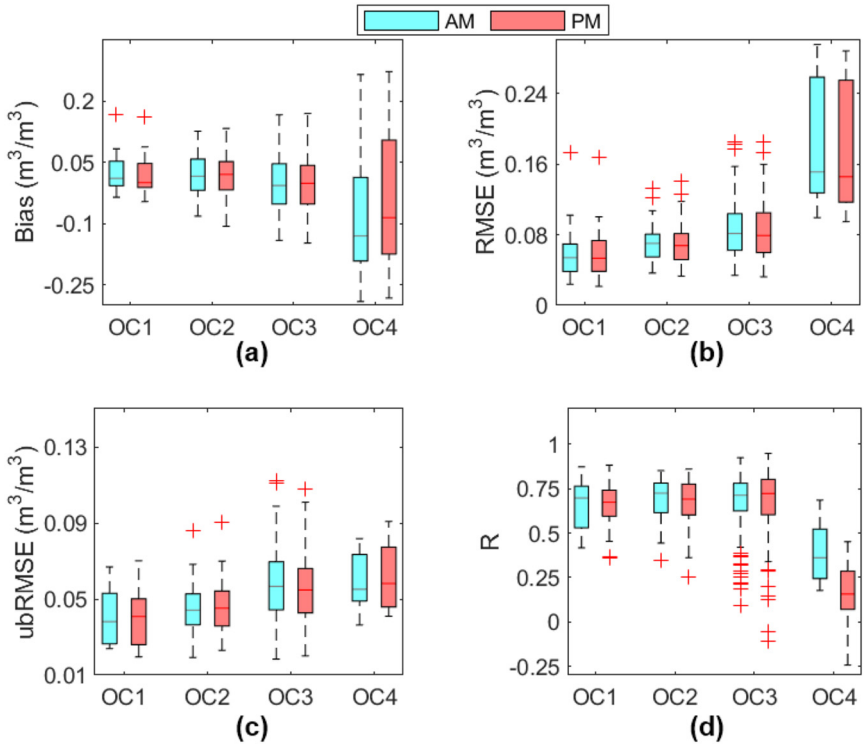

Fig. 4. SM assessments by four primary soil classes in terms of (a) bias, (b) RMSE, (c) ubRMSE and (d) R. (For interpretation of the references to color in this figure, the reader is referred to the web version of this article.)

from the box plots.

In general, it is also shown that the performance of AM product is slightly better than the PM product in the arid, temperate and cold zones, but differences in mean values of the metrics are not so statistically significant with large p values at some cases as presented in Table 6. However, it should be recognized that the 18 stations distributed over Polar zones (see Section 2.2.1) generally presents better performances in the PM product than those of the AM product while other climate zones tend to be opposite, which may be because of positive effects on the SM retrieval by mitigated freeze conditions resulting from higher temperature in the afternoon. This result suggests the performance of the AM product is not always better than that of the

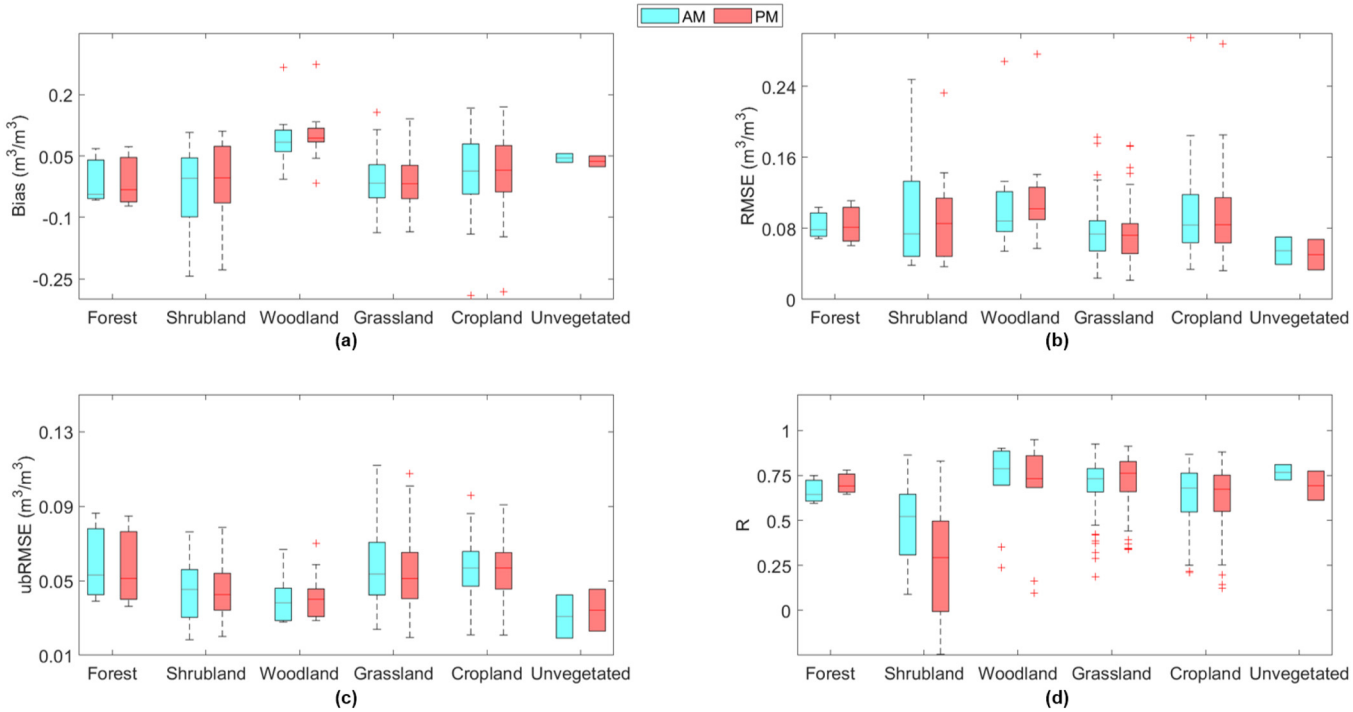

Fig. 5. Assessment results for the primary land covers in terms of (a) bias, (b) RMSE, (c) ubRMSE and (d) R. (For interpretation of the references to color in this figure, the reader is referred to the web version of this article.)

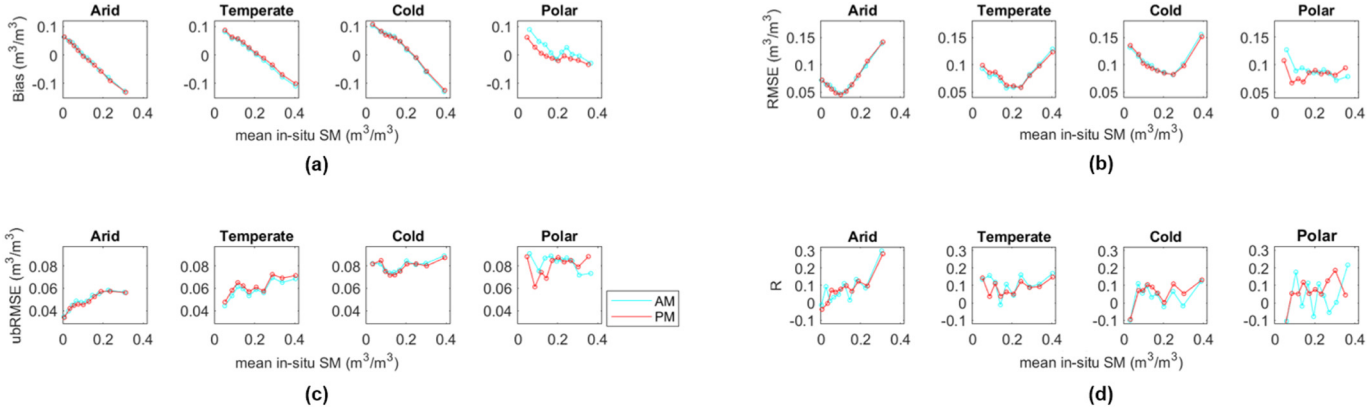

Fig. 6. Performance of SM retrievals with SW conditioned by CZ in terms of (a) bias (b) RMSE (c) ubRMSE and (d) R. (For interpretation of the references to color in this figure, the reader is referred to the web version of this article.)

PM product and more comprehensive consideration is necessary for the data selection based on physical and climatological conditions of the site.

As shown in Fig. 3a, the arid zones show underestimated biases, and those of the temperate zones are relatively closer to zero for both products. Fig. 3b–c show the RMSE and ubRMSE where the SM retrieval outperforms in the arid zones compared to others, which is possibly related to the lower vegetation attenuation. In case of R (Fig. 3d), highest R values are presented in the temperate and polar zones, but the cold zones show significant degradations compared to others. It has been noted that the brightness temperatures detected would decrease with increasing soil moisture or decreasing vegetation density (Monerris et al., 2003). When both soil moisture and vegetation density increase or decrease, the opposite effects can thereby occur on radiation signals leading to relatively larger differences between the SM retrievals and the ground measurements and these scenarios actually occur in different seasons (Gruhier et al., 2008). Therefore, the seasonally correlated trends of soil moisture and vegetation density may partly account for the relatively lower accuracy reported for the cold zones.

4.2.2. Soil property

Fig. 4 and Table 7 present assessment results with the four primary soil classes by organic carbon contents described in Section 2.2.2.

Generally, as presented by large *p* values in Table 7, except for a few cases, differences in mean values of the metrics for the AM and PM products are not so statistically significant along with the four primary soil classes, OC1-OC4. In addition, there are generally declining trends in the performances, except for R, with increasing soil organic carbon contents as shown in Fig. 4b–d. It is highlighted that the SMAP L3 products in OC4 class are highly degraded for all metrics compared to the cases of OC1 to OC3. Especially, the R values for OC4 are only around 0.2 with markedly lower reliability given the wide range of the boxes, with similar observations holding for the other metrics assessed as well. Even though the finding on OC4 cannot be concluded due to the lack of samples (8 stations), some reasons for this result can be formed. Firstly, it has been revealed that the increase in soil OC would decrease the soil bulk density and increase the fraction of bound water influencing the soil permittivity (Bircher et al., 2016; Jin et al., 2017; Jones et al., 2002; Jong et al., 1983; Malicki et al., 1996). According to Mironov and Bobrov (2003), the L-band refractive index for the agricultural soil samples (~0.16 m^3/m^3) containing 6.6% humus is lower than that of the soil samples (~0.15 m^3/m^3) with 0.6% humus which means the SM dielectric constants proportional to the soil reflectiveness are reduced as the increase of Soil OC. However, this relevant impact was not fully considered in Mironov et al. (2009) which is now applied to retrieve the version2 SMAP SM (Jackson et al., 2018) partially leading to the mis-match between the remotely-sensed products and the in-situ measurements. Based on the relative metrics here (ubRMSE and R), the current Mironov dielectric model used in SMAP SM retrieval may be not suitable for the zones with OC-rich soil (Jin et al., 2017). In addition, it should be noted that most stations of OC4 are located in the high latitude areas where the SM retrievals are difficult due to the effect of soil freezing and thaw process (Al-Yaari et al., 2014). Therefore, the poor R may be mainly attributed to that reason, given the surrounding stations with similar latitudes to those OC4 stations also present relatively poor performance in the specific validation. In the previous validation studies for the SMOS products, R values in high-latitude zones are also far lower than that in the other zones (Al-Yaari et al., 2014).

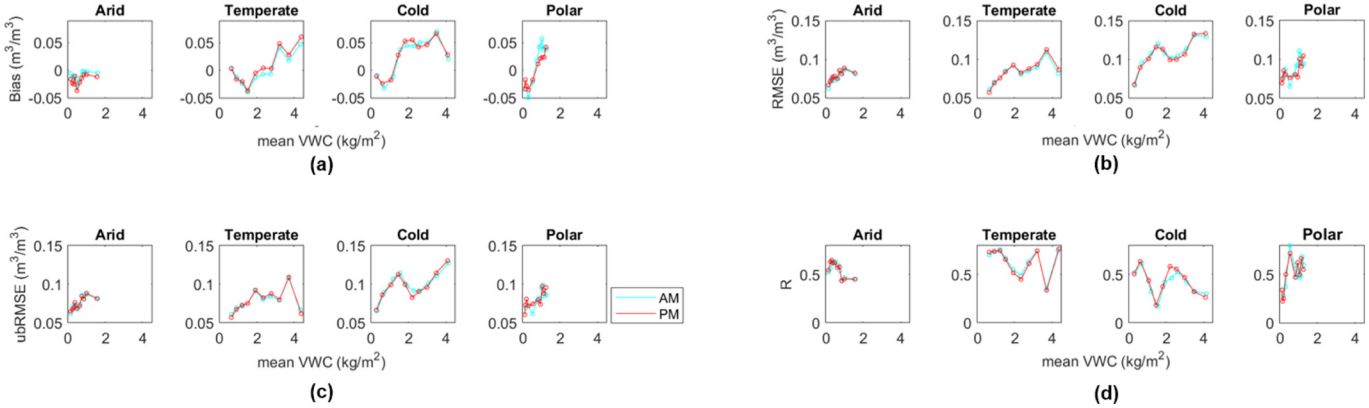

Fig. 7. Performance of SM retrievals with VD conditioned by CZ in terms of (a) bias (b) RMSE (c) ubRMSE and (d) R. (For interpretation of the references to color in this figure, the reader is referred to the web version of this article.)

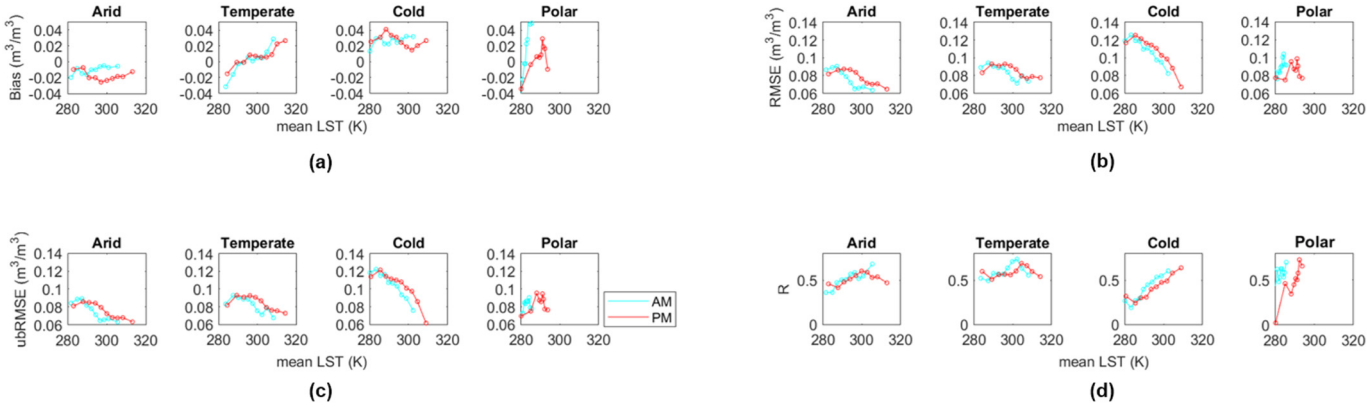

Fig. 8. Performance of SM retrievals with LST conditioned by CZ in terms of (a) bias (b) RMSE (c) ubRMSE and (d) R. (For interpretation of the references to color in this figure, the reader is referred to the web version of this article.)

Furthermore, three OC4 stations are from the FMI network (see Fig. 1 and Table 2) where the SM retrievals may also be affected by the presence of marshland or water bodies in addition to the Soil OC and high latitude (Al-Yaari et al., 2014).

4.2.3. Land cover

Fig. 5 and Table 8 present validation metrics for the six primary land cover classes. When considering the results for the forest and unvegetated regions, it is to be kept in mind that the number of stations for these land cover types are not enough (3 and 2 respectively).

In the grassland region, statistically significant differences in mean values of the metrics between the AM and PM products where small *p* values in Table 8. Apart from the forest and unvegetated regions due to lack of stations, negative biases (i.e. underestimation) are generally observed in the shrubland and grassland whereas results for the woodland and cropland tend to be positive (i.e. overestimation) (Fig. 5a), and the grassland generally presents lower RMSE than others (Fig. 5b). In terms of ubRMSE (Fig. 5c), the cropland shows relatively poorer performance than others which is consistent with the recent validation study for Version 2 SMAP product (Jackson et al., 2018) and possibly due to conspicuous seasonal variations in Cropland by either harvest or bare soil periods (Kim, 2013). Fig. 5d presents R values which are clearly different between the shrubland and grassland regions mainly distributed over the arid, semi-arid and temperate zones (Geruo et al., 2017). In fact, these differences in R values over the shrubland and grassland have been also observed in previous validation studies for the SMAP enhanced products using in-situ measurements from sparse networks (Chan et al., 2018; Jackson et al., 2018) where R values in the shrubland are significantly lower than those of the grassland. This could result from variabilities in native vegetation types for both areas, with the grassland considered more homogeneous compared to the shrubland (Neave and Abrahams, 2002). In addition, the sensitivity of vegetation in Shrubland to soil variations decreases whereas the grassland becomes more sensitive to the alterations in soil moisture conditions during drought periods (Geruo et al., 2017). While data was limited, overall performance for Unvegetated regions is relatively high which has been also reported from previous validation studies for passive L-band-derived SM products (Al-Yaari et al., 2014; Jackson et al., 2018).

4.3. Assessment results for dynamic factors conditioned by climate zones

In this section, assessment results with the dynamic factors, SW, VD and LST (see Section 2.3 for details), conditioned by the four primary climate zones (i.e. Arid, Temperate, Cold and Polar) are presented. Table 9 presents the total number of observations for each class used for calculating the statistical metrics presented through Figs. 6 to 8. Note that the results from the single station in the tropical region were excluded from the following result presentation.

4.3.1. Soil wetness

Fig. 6 presents the evaluation results of the SM retrievals' accuracy with SW conditioned by CZ.

First, the biases (Fig. 6a) in these four zones commonly reduce from positive to negative values with increasing SW. Here, the polar zone presents lower reduction rates and more distinguishable trends between the AM and PM products than other zones. In case of RMSE (Fig. 6b), the trends lines for the arid, temperate and cold zones show convex shapes for which stationary points with minimum RMSE values range from 0.1(for arid) to 0.2 m^3/m^3 (for temperate and cold). In the polar zone, RMSE values decrease with increasing SW but tends to be stable for SW > 0.1 m^3/m^3. In addition, the PM product in the polar zone generally shows lower RMSE than the AM product, which in line with the findings in Section 4.2.1. While the ubRMSE values, as presented in Fig. 6c, are stratified as low to high following with the arid, temperate and cold zones, those of the polar zone are significantly fluctuated with SW variability. Lastly, as shown in Fig. 6d, whereas R values in the arid zone generally increase with increasing SW, those for other zones are increased by the changing SW. Like the case of ubRMSE, the polar zone presents highly fluctuating patterns of R.

4.3.2. Vegetation density

The performance of SM retrievals with VD conditioned by CZ are shown in Fig. 7.

Overall, as presented in Fig. 7, while VD (i.e. mean VWC) values over the temperate and cold zones generally range 0.2 to 4.4 kg/m^2, those of the arid and polar zones are distributed in a narrower range, 0 to 2 kg/m^2. Biases (Fig. 7a) for the temperate and cold gradually increase from negative (dry bias, underestimation) to positive (wet bias,

Table 5
Summarised performance metrics for the AM and PM products.

Item	No. of stations	Bias	RMSE	ubRMSE	R
AM	191	0.001 ± 0.076	0.086 ± 0.041	0.055 ± 0.018	0.667 ± 0.171
PM	191	0.001 ± 0.076	0.085 ± 0.041	0.054 ± 0.018	0.651 ± 0.209
p value		0.763	0.264	0.002	0.028

Table 6
Summarised performance metrics of the AM and PM products by primary climate zones.

Climate zones	No. of stations	Item	Bias	RMSE	ubRMSE	R
Tropical	1	AM	−0.049	0.070	0.051	0.770
		PM	−0.067	0.084	0.050	0.783
		p value	–	–	–	–
Arid	58	AM	−0.015 ± 0.056	0.073 ± 0.029	0.050 ± 0.017	0.700 ± 0.123
		PM	−0.020 ± 0.057	0.072 ± 0.032	0.048 ± 0.017	0.693 ± 0.132
		p value	0.013	0.693	0.088	0.399
Temperate	35	AM	0.001 ± 0.061	0.078 ± 0.027	0.053 ± 0.019	0.750 ± 0.136
		PM	0.005 ± 0.064	0.079 ± 0.029	0.052 ± 0.019	0.731 ± 0.147
		p value	0.037	0.251	0.503	0.017
Cold	79	AM	0.011 ± 0.095	0.100 ± 0.051	0.056 ± 0.017	0.590 ± 0.184
		PM	0.015 ± 0.093	0.099 ± 0.050	0.056 ± 0.017	0.547 ± 0.245
		p value	0.177	0.380	0.396	0.005
Polar	18	AM	0.016 ± 0.058	0.088 ± 0.029	0.069 ± 0.018	0.733 ± 0.178
		PM	0.000 ± 0.058	0.081 ± 0.031	0.064 ± 0.016	0.805 ± 0.116
		p value	0.061	0.028	0.001	0.005
Total	191					

overestimation) values with increasing VD. However, Arid generally presents negative values with a small variability and those of the polar zone expeditiously increase over the narrow ranges of VD. These trends of biases with varied VD are similarly propagated into the cases of RMSE and ubRMSE as shown in Fig. 7b and c. In other words, RMSE and ubRMSE over the four CZs broadly increase with increasing VD in which the cold zone presents the most significant increases. In terms of R (Fig. 7d), the arid, temperate and cold zones generally present declining R values with increasing VD even though there are high variabilities whereas the polar zone tends to present higher R values with higher VD.

4.3.3. Land surface temperature

The performance of the SMAP with LST conditioned by CZ are presented in Fig. 8.

As shown in Fig. 8, compared to the cases of SW and VD, the performance trends with LST changes are clearly contrasted in the AM and PM products, in which the AM product has 5 to 6 K shorter LST ranges in the upper limits than the PM product. In addition, as LST increase, the performances of both products tend to be better in general. Here, it is to be noted that the AM product presents better performances than the PM product over the LST ranges in the arid, temperate and cold zones, but opposite trends (i.e. PM is better than AM) are observed in the polar zone having much shorter LST ranges than others. With respect to the bias (Fig. 8a), the SM retrievals in the arid and cold zones are inclined to be underestimated (negative) and overestimated (positive) respectively whereas those of the temperate gradually increase from negative to positive across zero around 295 K, and the biases in the polar zone sharply increase with increasing LST from 280 to 295 K (285 K for AM). As shown in Fig. 8b–c, RMSE and ubRMSE generally decrease with increasing LST where the cold zone shows clearly steeper trends than others, and the arid and temperate zones generally show better performances than the cold zone with RMSE and ubRMSE values. Similarly, R values tend to increase with increasing LST in which the arid and temperate present higher R values than others, and the cold and polar zones show precipitous inclines in their R values.

4.4. Caveats and follow-up studies

Despite the variation in performance across the six physical and climatological, it should be noted that the results here were constrained due to the spatiotemporal extent of the data that was available to this study. First, the ground stations from the sparse networks covering the first three-year of the SMAP observations were highly concentrated on the United States and Europe, and therefore performance gaps for the SM retrievals in some conditions cannot be fully explained due to lack of stations. More effective and globally distributed in-situ measurements can help improve the assessment accuracy further. Second, although one ground station from the sparse network is likely to reflect the temporal variability of the SM state within that grid, the spatial representativeness for the areal SM and the physical and climatological conditions used in this study in a $0.1^\circ \times 0.1^\circ$ pixel cannot be achieved by in-situ measurements from a single station. Moreover, the mis-match between the SM retrievals and the in-situ measurements from the sparse networks can also lead to more errors in the assessment results. Although we applied a strict filtering processes (Section 2.1.2), it should be noted that possibly remaining systematic differences among the datasets are somewhat arbitrary and can likely lead to unreliable assessment results, especially for metrics such as bias and RMSE. Therefore, the performance of SMAP products assessed using the sparse

Table 7
Summarised performance metrics of the AM and PM products by four primary soil classes.

Soil classes	No. of stations	Item	Bias	RMSE	ubRMSE	R
OC1	14	AM	0.026 ± 0.055	0.063 ± 0.039	0.041 ± 0.015	0.674 ± 0.143
		PM	0.022 ± 0.056	0.063 ± 0.038	0.041 ± 0.015	0.645 ± 0.162
		p value	0.115	0.800	0.973	0.123
OC2	25	AM	0.020 ± 0.054	0.071 ± 0.025	0.046 ± 0.014	0.691 ± 0.126
		PM	0.016 ± 0.058	0.071 ± 0.028	0.046 ± 0.015	0.675 ± 0.142
		p value	0.052	0.866	0.710	0.230
OC3	144	AM	0.000 ± 0.069	0.086 ± 0.033	0.058 ± 0.018	0.678 ± 0.168
		PM	−0.002 ± 0.071	0.085 ± 0.034	0.056 ± 0.017	0.675 ± 0.188
		p value	0.221	0.296	0.000	0.616
OC4	8	AM	−0.080 ± 0.181	0.183 ± 0.076	0.059 ± 0.016	0.389 ± 0.174
		PM	−0.040 ± 0.188	0.177 ± 0.077	0.062 ± 0.018	0.154 ± 0.208
		p value	0.221	0.231	0.415	0.060
Total	191					

Table 8
Summarised performance metrics of the AM and PM products by primary land cover classes.

Land cover classes	No. of stations	Item	Bias	RMSE	ubRMSE	R
Forest	3	AM	−0.011 ± 0.069	0.084 ± 0.018	0.059 ± 0.024	0.663 ± 0.079
		PM	−0.011 ± 0.075	0.084 ± 0.025	0.057 ± 0.025	0.706 ± 0.068
		p value	0.966	0.886	0.033	0.268
Shrubland	12	AM	−0.031 ± 0.101	0.096 ± 0.062	0.045 ± 0.018	0.483 ± 0.235
		PM	−0.009 ± 0.099	0.093 ± 0.055	0.046 ± 0.018	0.266 ± 0.326
		p value	0.305	0.540	0.738	0.013
Woodland	10	AM	0.094 ± 0.071	0.109 ± 0.061	0.040 ± 0.012	0.709 ± 0.232
		PM	0.102 ± 0.073	0.117 ± 0.061	0.042 ± 0.014	0.655 ± 0.291
		p value	0.127	0.017	0.500	0.048
Grassland	88	AM	−0.013 ± 0.055	0.077 ± 0.030	0.057 ± 0.020	0.703 ± 0.145
		PM	−0.018 ± 0.054	0.075 ± 0.031	0.054 ± 0.019	0.724 ± 0.139
		p value	0.025	0.057	0.000	0.004
Cropland	76	AM	0.010 ± 0.085	0.094 ± 0.043	0.057 ± 0.015	0.647 ± 0.164
		PM	0.010 ± 0.085	0.093 ± 0.044	0.056 ± 0.015	0.623 ± 0.176
		p value	0.905	0.528	0.218	0.000
Unvegetated	2	AM	0.045 ± 0.015	0.055 ± 0.022	0.031 ± 0.016	0.767 ± 0.060
		PM	0.037 ± 0.018	0.050 ± 0.024	0.034 ± 0.016	0.693 ± 0.115
		p value	0.168	0.246	0.061	0.305
Total	191					

Table 9
Number of observations for four primary climate zone classes.

Product	Arid	Temperate	Cold	Polar	Total
AM	21,061	11,592	24,283	2178	59,114
PM	21,453	11,680	25,816	2504	61,453

network cannot fully reflect their accuracy even though it is likely to follow similar pattern to the evaluation metrics using the CVSs based on the previous validation results (Chan et al., 2018; Jackson et al., 2018). Hence, the relative metrics such as ubRMSE and R have a higher weight in the quality evaluation in this study.

It should be also recognized that there may be complex interdependencies among the rough six physical and climatological conditions considered in this study and that there may be other important factors significantly affecting the SM retrieval that are not investigated here (i.e. surface roughness, soil fraction, water fraction and so on). Many other sub-classifications could not be considered due to the limited ground coverage that was available. In this regard, this study examines the sensitivity of the SM product performance for a few given conditions, rather than considering the actual combination of conditions. Considering the difficulty of completely investigating the interdependency among all possible conditions related to the SM retrieval, this paper makes some meaningful steps towards improving the SMAP L3 product. The authors hope that this paper will provide clues on the improvements and guidelines for users.

5. Conclusions

This study comprehensively evaluated the 3-year version 2 SMAP Enhanced L3 Radiometer soil moisture product (Version 2) by comparing with in-situ measurements from 191 stations distributed over various physical and climatological conditions across the world. Based on four assessment metrics (i.e. bias, RMSE, ubRMSE and R), the following findings can be reported.

1. The descending (AM) product was generally found to be better than the ascending (PM) product, without significant differences between the two products being present. This supports the argument that the PM product can be used for various applications together with the AM product, unlike the approach that has been adopted in previous missions (Section 4.1). However, 18 stations distributed over Polar zones generally presents higher R values in the PM product which is opposite to the general recognition suggesting more comprehensive consideration is necessary for selecting the SMAP SM data based on site conditions (Section 4.2.1).
2. The SMAP product generally showed better performances in Arid and Temperate zones than in Cold zones (Sections 4.2 and 4.3).
3. Declining performances were observed with increasing soil organic carbon (OC) contents. Especially, significant degradations for all metrics were observed in OC4 class where soil organic carbon is > 8.74%. Reasons for this should be carefully evaluated and retrieval algorithms modified to improve accuracy for this class. Consideration needs to be given for any applications of the retrieved products over such zones as well (Section 4.2.2).
4. Of the two dominant land cover types, grassland and cropland, the former generally showed better performances (Section 4.2.3).
5. In the assessments with dynamic factors conditioned by the climate zones (Section 4.3), better performances were found in arid followed by temperate and finally cold zones at lower SW and VD, and higher LST. The temperate zone generally presented gradual transitions in the performances with changes in the dynamic factors while those of the arid and cold zones are relatively dull. Meanwhile, the polar zones can be characterized by 1) better performances in the PM product, 2) high fluctuations in the performances with changes in the dynamic factors, and 3) steeper trends than other climate zones.
6. In general, the performance of the SM retrievals from the dataset are fairly good in terms of bias and temporal correlation against the in-situ measurements, while also being mostly better than satellite products derived from previous missions (Cui et al., 2018; H. Kim et al., 2018).

In the absence of the continuously long-term ground measurements across the world, the performance of surface SM retrievals cannot be evaluated thoroughly. However, the results here offer an assessment that maximizes the use of the existing relevant data and can serve as an appropriate reference for further investigations as more data becomes available.

Acknowledgements

This work has been undertaken as part of a Discovery Project (DP180102737) funded by the Australian Research Council. We are grateful to all contributors to the datasets used in this study.

Appendix A. Supplementary data

Supplementary data to this article can be found online at https://doi.org/10.1016/j.rse.2019.01.015.

References

Albergel, C., Rüdiger, C., Pellarin, T., Calvet, J.-C., Fritz, N., Froissard, F., Suquia, D., Petitpa, A., Piguet, B., Martin, E., 2008. From near-surface to root-zone soil moisture using an exponential filter: an assessment of the method based on in-situ observations and model simulations. Hydrol. Earth Syst. Sci. 12, 1323–1337.

Al-Yaari, A., Wigneron, J.-P., Ducharne, A., Kerr, Y., De Rosnay, P., De Jeu, R., Govind, A., Al Bitar, A., Albergel, C., Munoz-Sabater, J., 2014. Global-scale evaluation of two satellite-based passive microwave soil moisture datasets (SMOS and AMSR-E) with respect to Land Data Assimilation System estimates. Remote Sens. Environ. 149, 181–195.

Al-Yaari, A., Wigneron, J.-P., Kerr, Y., Rodriguez-Fernandez, N., O'Neill, P., Jackson, T., De Lannoy, G., Al Bitar, A., Mialon, A., Richaume, P., 2017. Evaluating soil moisture retrievals from ESA's SMOS and NASA's SMAP brightness temperature datasets. Remote Sens. Environ. 193, 257–273.

Bell, J.E., Palecki, M.A., Baker, C.B., Collins, W.G., Lawrimore, J.H., Leeper, R.D., Hall, M.E., Kochendorfer, J., Meyers, T.P., Wilson, T., 2013. US Climate Reference Network soil moisture and temperature observations. J. Hydrometeorol. 14, 977–988.

Bertoldi, G., Della Chiesa, S., Notarnicola, C., Pasolli, L., Niedrist, G., Tappeiner, U., 2014. Estimation of soil moisture patterns in mountain grasslands by means of SAR RADARSAT2 images and hydrological modeling. J. Hydrol. 516, 245–257.

Beven, K., Fisher, J., 1996. Remote sensing and scaling in hydrology. In: Stewart, J.B., Engman, E.T., Feddes, A., Kerr, Y. (Eds.), Scaling in Hydrology Using Remote Sensing. Wiley, New York, pp. 93–111.

Bindlish, R., Jackson, T., Cosh, M., Zhao, T., O'neill, P., 2015. Global soil moisture from the Aquarius/SAC-D satellite: Description and initial assessment. IEEE Geosci. Remote Sens. Lett. 12, 923–927.

Bircher, S., Skou, N., Jensen, K.H., Walker, J.P., Rasmussen, L., 2012. A soil moisture and temperature network for SMOS validation in Western Denmark. Hydrol. Earth Syst. Sci. 16, 1445–1463.

Bircher, S., Demontoux, F., Razafindratsima, S., Zakharova, E., Drusch, M., Wigneron, J.-P., Kerr, Y.H., 2016. L-band relative permittivity of organic soil surface layers—a new dataset of resonant cavity measurements and model evaluation. Remote Sens. 8, 1024.

Brodzik, M.J., Billingsley, B., Haran, T., Raup, B., Savoie, M.H., 2012. EASE-Grid 2.0: incremental but significant improvements for Earth-gridded data sets. ISPRS Int. J. Geo-Inf. 1, 32–45.

Burgin, M.S., Colliander, A., Njoku, E.G., Chan, S.K., Cabot, F., Kerr, Y.H., Bindlish, R., Jackson, T.J., Entekhabi, D., Yueh, S.H., 2017. A comparative study of the SMAP passive soil moisture product with existing satellite-based soil moisture products. IEEE Trans. Geosci. Remote Sens. 55, 2959–2971.

Chan, S., 2016. Enhanced Level 3 Passive Soil Moisture Product Specification Document.

Chan, S., Hunt, R., Bindlish, R., Njoku, E., Kimball, J., Jackson, T., 2013. SMAP Ancillary Data Report: Vegetation Water Content. Jet Propulsion Lab., California Inst. Technol., Pasadena, CA, USA (JPL D-53058).

Chan, S.K., Bindlish, R., O'Neill, P.E., Njoku, E., Jackson, T., Colliander, A., Chen, F., Burgin, M., Dunbar, S., Piepmeier, J., 2016. Assessment of the SMAP passive soil moisture product. IEEE Trans. Geosci. Remote Sens. 54, 4994–5007.

Chan, S., Bindlish, R., O'Neill, P., Jackson, T., Njoku, E., Dunbar, S., Chaubell, J., Piepmeier, J., Yueh, S., Entekhabi, D., 2018. Development and assessment of the SMAP enhanced passive soil moisture product. Remote Sens. Environ. 204, 931–941.

Chen, F., Crow, W.T., Starks, P.J., Moriasi, D.N., 2011. Improving hydrologic predictions of a catchment model via assimilation of surface soil moisture. Adv. Water Resour. 34, 526–536.

Chen, F., Crow, W.T., Colliander, A., Cosh, M.H., Jackson, T.J., Bindlish, R., Reichle, R.H., Chan, S.K., Bosch, D.D., Starks, P.J., 2017. Application of triple collocation in ground-based validation of Soil Moisture Active/Passive (SMAP) level 2 data products. IEEE J. Sel. Top. Appl. Earth Obs. Remote Sens. 10, 489–502.

Choudhury, B., Schmugge, T., Mo, T., 1982. A parameterization of effective soil temperature for microwave emission. J. Geophys. Res. Oceans Atmos. 87, 1301–1304.

Chung, D., Dorigo, W., De Jeu, R., Kidd, R., Wagner, W., 2018. ESA climate change initiative phase II - soil moisture product specification document (PSD) D1.2.1 Version 4.2. Earth Observation Data Centre for Water Resources Monitoring (EODC) GmbH.

Colliander, A., Cosh, M.H., Misra, S., Jackson, T.J., Crow, W.T., Chan, S., Bindlish, R., Chae, C., Collins, C.H., Yueh, S.H., 2017a. Validation and scaling of soil moisture in a semi-arid environment: SMAP validation experiment 2015 (SMAPVEX15). Remote Sens. Environ. 196, 101–112.

Colliander, A., Jackson, T., Bindlish, R., Chan, S., Das, N., Kim, S., Cosh, M., Dunbar, R., Dang, L., Pashaian, L., 2017b. Validation of SMAP surface soil moisture products with core validation sites. Remote Sens. Environ. 191, 215–231.

Colliander, A., Jackson, T.J., Chan, S., O'Neill, P., Bindlish, R., Cosh, M., Caldwell, T., Walker, J., Berg, A., McNairn, H., 2018. An assessment of the differences between spatial resolution and grid size for the SMAP enhanced soil moisture product over homogeneous sites. Remote Sens. Environ. 207, 65–70.

Crow, W.T., Berg, A.A., Cosh, M.H., Loew, A., Mohanty, B.P., Panciera, R., de Rosnay, P., Ryu, D., Walker, J.P., 2012. Upscaling sparse ground-based soil moisture observations for the validation of coarse-resolution satellite soil moisture products. Rev. Geophys. 50, RG2002.

Cui, C., Xu, J., Zeng, J., Chen, K.-S., Bai, X., Lu, H., Chen, Q., Zhao, T., 2018. Soil moisture mapping from satellites: an intercomparison of SMAP, SMOS, FY3B, AMSR2, and ESA CCI over two dense network regions at different spatial scales. Remote Sens. 10, 33.

Das, K., Paul, P.K., 2015. Present status of soil moisture estimation by microwave remote sensing. Cogent Geosci. 1, 1084669.

De Jeu, R., Wagner, W., Holmes, T., Dolman, A., Van De Giesen, N., Friesen, J., 2008. Global soil moisture patterns observed by space borne microwave radiometers and scatterometers. Surv. Geophys. 29, 399–420.

De Lannoy, G.J.M., Koster, R.D., Reichle, R.H., Mahanama, S.P.P., Liu, Q., 2014. An updated treatment of soil texture and associated hydraulic properties in a global land modeling system. J. Adv. Model. Earth Syst. 6, 957–979.

Dorigo, W., Wagner, W., Hohensinn, R., Hahn, S., Paulik, C., Xaver, A., Gruber, A., Drusch, M., Mecklenburg, S., Oevelen, P.v., 2011. The International Soil Moisture Network: a data hosting facility for global in situ soil moisture measurements. Hydrol. Earth Syst. Sci. 15, 1675–1698.

Dorigo, W., Xaver, A., Vreugdenhil, M., Gruber, A., Hegyiova, A., Sanchis-Dufau, A., Zamojski, D., Cordes, C., Wagner, W., Drusch, M., 2013. Global automated quality control of in situ soil moisture data from the International Soil Moisture Network. Vadose Zone J. 12.

Dorigo, W., Gruber, A., De Jeu, R., Wagner, W., Stacke, T., Loew, A., Albergel, C., Brocca, L., Chung, D., Parinussa, R., 2015. Evaluation of the ESA CCI soil moisture product using ground-based observations. Remote Sens. Environ. 162, 380–395.

Dorigo, W., Wagner, W., Albergel, C., Albrecht, F., Balsamo, G., Brocca, L., Chung, D., Ertl, M., Forkel, M., Gruber, A., Haas, E., Hamer, P.D., Hirschi, M., Ikonen, J., de Jeu, R., Kidd, R., Lahoz, W., Liu, Y.Y., Miralles, D., Mistelbauer, T., Nicolai-Shaw, N., Parinussa, R., Pratola, C., Reimer, C., van der Schalie, R., Seneviratne, S.I., Smolander, T., Lecomte, P., 2017. ESA CCI Soil Moisture for improved Earth system understanding: state-of-the art and future directions. Remote Sens. Environ. 203, 185–215.

Engda, T.A., Kelleners, T.J., 2016. Soil moisture-based drought monitoring at different time scales: a case study for the U.S. Great Plains. J. Am. Water Resour. Assoc. 52, 77–88.

Entekhabi, D., Njoku, E.G., O'Neill, P.E., Kellogg, K.H., Crow, W.T., Edelstein, W.N., Entin, J.K., Goodman, S.D., Jackson, T.J., Johnson, J., 2010a. The soil moisture active passive (SMAP) mission. Proc. IEEE 98, 704–716.

Entekhabi, D., Reichle, R.H., Koster, R.D., Crow, W.T., 2010b. Performance metrics for soil moisture retrievals and application requirements. J. Hydrometeorol. 11, 832–840.

Entekhabi, D., Yueh, S., O'Neill, P., Kellogg, K., Allen, A., Bindlish, R., Brown, M., Chan, S., Colliander, A., Crow, W., 2014. SMAP Handbook. JPL Publication JPL, pp. 400–1567.

Friedl, M.A., Sulla-Menashe, D., Tan, B., Schneider, A., Ramankutty, N., Sibley, A., Huang, X., 2010. MODIS collection 5 global land cover: algorithm refinements and characterization of new datasets. Remote Sens. Environ. 114, 168–182.

GCOS, 2006. Systematic Observation Requirements for Satellite-Based Products for Climate-Supplemental Details to the Satellite-Based Component of the "Implementation Plan for the Global Observing System for Climate in Support of the UNFCCC".

Geruo, A., Velicogna, I., Kimball, J.S., Du, J., Kim, Y., Colliander, A., Njoku, E., 2017. Satellite-observed changes in vegetation sensitivities to surface soil moisture and total water storage variations since the 2011 Texas drought. Environ. Res. Lett. 12, 054006.

Global Modeling and Assimilation Office (GMAO), 2015. MERRA-2 tavg1_2d_lnd_Nx: 2d,1-Hourly,Time-Averaged,Single-Level,Assimilation,Land Surface Diagnostics V5.12.4. Goddard Earth Sciences Data and Information Services Center (GES DISC), Greenbelt, MD, USAhttps://doi.org/10.5067/RKPHT8KC1Y1T, Accessed date: 9 October 2018.

Gruhier, C., De Rosnay, P., Kerr, Y., Mougin, E., Ceschia, E., Calvet, J.C., Richaume, P., 2008. Evaluation of AMSR-E soil moisture product based on ground measurements over temperate and semi-arid regions. Geophys. Res. Lett. 35.

Hunt, E.R., Piper, S.C., Nemani, R., Keeling, C.D., Otto, R.D., Running, S.W., 1996. Global net carbon exchange and intra-annual atmospheric CO2 concentrations predicted by an ecosystem process model and three-dimensional atmospheric transport model. Glob. Biogeochem. Cycles 10, 431–456.

Jackson, T.J., Bindlish, R., Cosh, M.H., Zhao, T., Starks, P.J., Bosch, D.D., Seyfried, M.S., Moran, M.S., Kerr, Y., Lerousx, D., 2012. Validation of soil moisture and ocean salinity (SMOS) soil moisture over watershed networks in the U.S. IEEE Trans. Geosci. Remote Sens. 1530–1543.

Jackson, T., O'Neill, P., S. C., Bindlish, R., Colliander, A., Chen, F., Burgin, M., Dunbar, S., Piepmeier, J., Cosh, M., Caldwell, T., Walker, J., Wu, X., Berg, A., Rowlandson, T., Pacheco, A., McNairn, H., Thibeault, M., Martínez-Fernández, J., González-Zamora, Á., Lopez-Baeza, E., Udall, F., Seyfried, M., Bosch, D., Starks, P., Holifield, C., Prueger, J., Su, Z., van der Velde, R., Asanuma, J., Palecki, M., Small, E., Zreda, M., Calvet, J., Crow, W., Kerr, Y., Yueh, S., Entekhabi, D., 2018. Calibration and Validation for the L2/3_SM_P Version 5and L2/3_SM_P_E Version 2 Data Products, SMAP Project, JPL D-56297. Jet Propulsion Laboratory, Pasadena, CA.

Jin, M., Zheng, X., Jiang, T., Li, X., Li, X.-J., Zhao, K., 2017. Evaluation and improvement of SMOS and SMAP soil moisture products for soils with high organic matter over a forested area in Northeast China. Remote Sens. 9, 387.

Jones, S.B., Wraith, J.M., Or, D., 2002. Time domain reflectometry measurement principles and applications. Hydrol. Process. 16, 141–153.

Jong, R.d., Campbell, C., Nicholaichuk, W., 1983. Water retention equations and their relationship to soil organic matter and particle size distribution for disturbed samples. Can. J. Soil Sci. 63, 291–302.

Kay, B., Silva, A.d., Baldock, J., 1997. Sensitivity of soil structure to changes in organic carbon content: predictions using pedotransfer functions. Can. J. Soil Sci. 77, 655–667.

Kerr, Y., Wigneron, J.-P., Al Bitar, A., Mialon, A., Srivastava, P., 2016. Soil moisture from space: techniques and limitations. In: Satellite Soil Moisture Retrieval. Elsevier, pp. 3–27.
Kim, S., 2013. SMAP Ancillary Data Report: Landcover Classification. Jet Propulsion Lab., California Inst. Technol., Pasadena, CA, USA (JPL D-53058).
Kim, S., Liu, Y.Y., Johnson, F.M., Parinussa, R.M., Sharma, A., 2015. A global comparison of alternate AMSR2 soil moisture products: why do they differ? Remote Sens. Environ. 161, 43–62.
Kim, H., Parinussa, R., Konings, A.G., Wagner, W., Cosh, M.H., Lakshmi, V., Zohaib, M., Choi, M., 2018. Global-scale assessment and combination of SMAP with ASCAT (active) and AMSR2 (passive) soil moisture products. Remote Sens. Environ. 204, 260–275.
Kim, S., Paik, K., Johnson, F.M., Sharma, A., 2018. Building a flood-warning framework for ungauged locations using low resolution, open-access remotely sensed surface soil moisture, precipitation, soil, and topographic information. IEEE J. Sel. Top. Appl. Earth Obs. Remote Sens. 11, 375–387.
Kornelsen, K.C., Coulibaly, P., 2013. Advances in soil moisture retrieval from synthetic aperture radar and hydrological applications. J. Hydrol. 476, 460–489.
Koster, R.D., Dirmeyer, P.A., Guo, Z., Bonan, G., Chan, E., Cox, P., Gordon, C., Kanae, S., Kowalczyk, E., Lawrence, D., 2004. Regions of strong coupling between soil moisture and precipitation. Science 305, 1138–1140.
Leavesley, G., David, O., Garen, D., Lea, J., Marron, J., Pagano, T., Perkins, T., Strobel, M., 2008. A Modeling Framework for Improved Agricultural Water Supply Forecasting. (AGU Fall Meeting Abstracts).
Letts, M.G., Roulet, N.T., Comer, N.T., Skarupa, M.R., Verseghy, D.L., 2000. Parametrization of peatland hydraulic properties for the Canadian Land Surface Scheme. Atmosphere-Ocean 38, 141–160.
Li, Y., Grimaldi, S., Pauwels, V.R.N., Walker, J.P., 2018. Hydrologic model calibration using remotely sensed soil moisture and discharge measurements: the impact on predictions at gauged and ungauged locations. J. Hydrol. 557, 897–909.
Malicki, M., Plagge, R., Roth, C., 1996. Improving the calibration of dielectric TDR soil moisture determination taking into account the solid soil. Eur. J. Soil Sci. 47, 357–366.
Manns, H.R., Berg, A.A., Bullock, P.R., McNairn, H., Groenevelt, P., Yang, W., 2017. Importance of soil organic carbon in near-surface soil water content estimation: a simple model comparison in dry-end Canadian Prairie soils. Can. Water Res. J. 42, 364–377.
Mironov, V.L., Bobrov, P.P., 2003. Soil dielectric spectroscopic parameters dependence on humus content. In: Geoscience and Remote Sensing Symposium, 2003. IGARSS'03. Proceedings. 2003 IEEE International. IEEE, pp. 1106–1108.
Mironov, V.L., Kosolapova, L.G., Fomin, S.V., 2009. Physically and mineralogically based spectroscopic dielectric model for moist soils. IEEE Trans. Geosci. Remote Sens. 47, 2059–2070.
Mo, T., Choudhury, B.J., Schmugge, T.J., Wang, J.R., Jackson, T.J., 1982. A model for microwave emission from vegetation-covered fields. J. Geophys. Res. Oceans 87, 11229–11237.
Moghaddam, M., Entekhabi, D., Goykhman, Y., Li, K., Liu, M., Mahajan, A., Nayyar, A., Shuman, D., Teneketzis, D., 2010. A wireless soil moisture smart sensor web using physics-based optimal control: concept and initial demonstrations. IEEE J. Sel. Top. Appl. Earth Obs. Remote Sens. 3, 522–535.
Monerris, A., Vall-llossera, M., Camps, A., 2003. Study of Soil Moisture Retrieval Algorithms Using Multi-angular L-Band Brightness Temperatures: Application to ESA's SMOS Earth Explorer Opportunity Mission.
Nachtergaele, F., Batjes, N., 2012. Harmonized World Soil Database. FAO.
Neave, M., Abrahams, A.D., 2002. Vegetation influences on water yields from grassland and shrubland ecosystems in the Chihuahuan Desert. Earth Surf. Process. Landf. 27, 1011–1020.
NRCS Soil Survey Staff, U., 2012. General Soil Map (STATSGO2). ((United States), Washington, D.C. In).
Ochsner, T.E., Cosh, M.H., Cuenca, R.H., Dorigo, W.A., Draper, C.S., Hagimoto, Y., Kerr, Y.H., Njoku, E.G., Small, E.E., Zreda, M., 2013. State of the art in large-scale soil moisture monitoring. Soil Sci. Soc. Am. J. 77, 1888–1919.
Ojo, E.R., Bullock, P.R., L'Heureux, J., Powers, J., McNairn, H., Pacheco, A., 2015. Calibration and evaluation of a frequency domain reflectometry sensor for real-time soil moisture monitoring. Vadose Zone J. 14.
O'Neill, P., Chan, S., Njoku, E., Jackson, T., Bindlish, R., 2016a. SMAP Enhanced L3 Radiometer Global Daily 9 km EASE-Grid Soil Moisture, Version 1. NASA National Snow and Ice Data Center Distributed Active Archive Center.
O'Neill, P., Njoku, E., Jackson, T., Chan, S., Bindlish, R., 2016b. SMAP Algorithm Theoretical Basis Document: Level 2 & 3 Soil Moisture (Passive) Data Products. Jet Propulsion Lab., California Inst. Technol., Pasadena, CA, USA (JPL D-66480).
Pan, M., Cai, X., Chaney, N.W., Entekhabi, D., Wood, E.F., 2016. An initial assessment of SMAP soil moisture retrievals using high-resolution model simulations and in situ observations. Geophys. Res. Lett. 43, 9662–9668.
Parinussa, R.M., Meesters, A.G.C.A., Liu, Y., Dorigo, W., Wagner, W., De Jeu, R.A.M., 2011. Error estimates for near-real-time satellite soil moisture as derived from the land parameter retrieval model. IEEE Geosci. Remote Sens. Lett. 8, 779–783.
Peel, M.C., Finlayson, B.L., McMahon, T.A., 2007. Updated world map of the Köppen-Geiger climate classification. Hydrol. Earth Syst. Sci. Discuss. 4, 439–473.
Petropoulos, G.P., Ireland, G., Barrett, B., 2015. Surface soil moisture retrievals from remote sensing: current status, products & future trends. Phys. Chem. Earth A/B/C 83, 36–56.
Piepmeier, J.R., Johnson, J.T., Mohammed, P.N., Bradley, D., Ruf, C., Aksoy, M., Garcia, R., Hudson, D., Miles, L., Wong, M., 2014. Radio-frequency interference mitigation for the soil moisture active passive microwave radiometer. IEEE Trans. Geosci. Remote Sens. 52, 761–775.
Sanchez, N., Martinez-Fernandez, J., Scaini, A., Perez-Gutierrez, C., 2012. Validation of the SMOS L2 soil moisture data in the REMEDHUS Network (Spain). IEEE Trans. Geosci. Remote Sens. 50, 1602–1611.
Schmugge, T.J., 1980. Effect of texture on microwave emission from soils. IEEE Trans. Geosci. Remote Sens. GE-18, 353–361.
SMAP Algorithm Development Team, SMAP Science Team, 2015. Soil Moisture Active Passive (SMAP) Ancillary Data Report Surface Temperature. (In).
Srivastava, P., Pandey, V., Suman, S., Gupta, M., Islam, T., 2016. Chapter 2-Available Data Sets and Satellites for Terrestrial Soil Moisture Estimation, Satellite Soil Moisture Retrieval. Elsevier, In.
Ulaby, F.T., Moore, R.K., Fung, A.K., 1986. Microwave Remote Sensing Active and Passive-Volume III: From Theory to Applications.
Wigneron, J.P., Jackson, T.J., O'Neill, P., De Lannoy, G., de Rosnay, P., Walker, J.P., Ferrazzoli, P., Mironov, V., Bircher, S., Grant, J.P., Kurum, M., Schwank, M., Munoz-Sabater, J., Das, N., Royer, A., Al-Yaari, A., Al Bitar, A., Fernandez-Moran, R., Lawrence, H., Mialon, A., Parrens, M., Richaume, P., Delwart, S., Kerr, Y., 2017. Modelling the passive microwave signature from land surfaces: a review of recent results and application to the L-band SMOS & SMAP soil moisture retrieval algorithms. Remote Sens. Environ. 192, 238–262.
Yang, K., Qin, J., Zhao, L., Chen, Y., Tang, W., Han, M., Lazhu, Chen, Z., Lv, N., Ding, B., Wu, H., Lin, C., 2013. A multiscale soil moisture and freeze–thaw monitoring network on the third pole. Bull. Am. Meteorol. Soc. 94, 1907–1916.
Zhang, X., Zhang, T., Zhou, P., Shao, Y., Gao, S., 2017. Validation analysis of SMAP and AMSR2 soil moisture products over the United States using ground-based measurements. Remote Sens. 9, 104.
Zreda, M., Desilets, D., Ferré, T.P.A., Scott, R.L., 2008. Measuring soil moisture content non-invasively at intermediate spatial scale using cosmic-ray neutrons. Geophys. Res. Lett. 35, L21402.